RSC Advances

ROYAL SOCIETY OF CHEMISTRY

www.rsc.org/advances

Graphic Abstract

Novel pyridinium-based ionic liquids [NEt_2C_2Py][SCN], [C_4OPy][SCN] and [C_4CNPy][SCN] with high SO_2 gravimetric capacity were developed and the mechanism was discussed.

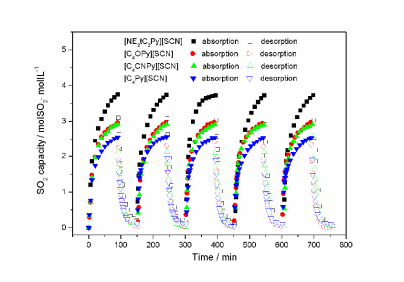

Improving SO_2 Capture by Tuning Functional Groups on the Cation of Pyridinium-based Ionic Liquids

Shaojuan Zeng [a, b], Hongyan He [a], Hongshuai Gao [a], Xiangping Zhang [*, a], Jian Wang [a, b], Ying Huang [a, b], Suojiang Zhang [*, a]

Abstract: In this work, three kinds of novel functionalized ionic liquids (ILs) $[NEt_2C_2Py][SCN]$, $[C_4OPy][SCN]$ and $[C_4CNPy][SCN]$ were developed by introducing a tertiary amino group, ether group and nitrile group on the pyridinium cation to improve SO_2 absorption performances. Among the investigated ILs, $[NEt_2C_2Py][SCN]$ showed the highest absorption capacity of 1.06 $gSO_2 \cdot gIL^{-1}$ under ambient conditions due to a combination of the chemical and physical absorption. By contrast, the enhancement in SO_2 capacity by $[C_4CNPy][SCN]$ and $[C_4OPy][SCN]$ is mainly ascribed to the stronger physical interaction between ILs and SO_2 than the conventional IL $[C_4Py][SCN]$. Meanwhile, higher SO_2/CO_2 selectivity was also obtained using these functionalized ILs, which was increased up to 41% comparing with that of $[C_4Py][SCN]$. Moreover, the effect of water on SO_2 capacity and the absorption mechanism were studied. The results indicated that the presence of water caused a slight decrease in SO_2 capacity of $[C_4CNPy][SCN]$ and $[C_4OPy][SCN]$ because of physical absorption, whereas a slight increase in SO_2 capacity by $[NEt_2C_2Py][SCN]$ due to the formation of hydrogen sulfite salts through chemical absorption. In addition, three kinds of cation-functionalized ILs could remain the stable absorption performance after five cycles of absorption and desorption, implying these ILs show great potentials for SO_2 capture.

Keywords: pyridinium, ionic liquids, sulfur dioxide, separation, cation-functionalized

1. Introduction

The increasing emission of SO_2 from the combustion of fossil fuels has inevitably brought about very adverse influences on environmental issues and human health. Up to now, some traditional methods for flue gas desulfurization (FGD) have been developed, such as limestone scribbling, ammonia scribbling and organic amines scribbling[1-3]. Among them, although limestone scribbling as one of the most attractive approaches has been applied widely in industries, this irreversible process usually results in huge amounts of byproducts and wastewater that doesn't comply with the sustainable principles. For amine scrubbing that can efficiently minimize additional pollutants and recover SO_2, yet they also possess inherent drawbacks, such as the loss of solvents due to their high volatility and degradation as well as high energy consumption for regeneration[4-7]. Therefore, the design and development of a proper absorbent for efficient and reversible capture of SO_2 is of critical importance in the absorption process.

Recently, ionic liquids (ILs) have drawn extensive attentions as competitive candidates in the field of acidic gases (CO_2[8-15], SO_2[16-23], and so on) capture and separation owing to their unique properties, such as extremely low vapour pressure, high thermal stability and tuneable properties[24-26]. It was reported that in general SO_2 has optimistic physical solubility in conventional ILs, and compared with the cation of ILs the anion plays a primary role in SO_2 capture[27-29]. Therefore, a great number of anion-functionalized ILs, such as azole-based ILs[30-33], benzoate and

phenolate-based ILs with halogen groups[34], dicarboxylic acid-based ILs[35, 36], lactate-based ILs[37], acetate-based ILs[38], phosphate-based ILs[39], were designed and synthesized for enhanced SO_2 capture by introducing different interaction sites on the anions. Among them, the phenyl-containing azole-based ILs showed the highest capacity of SO_2 absorption, which could reach 5.75 molSO_2·molIL^{-1} (0.61 gSO_2·gIL^{-1}) at 20℃ and 0.1MPa. However, there are very few types of cation-functionalized ILs for SO_2 capture, which mainly focused on ether-functionalized ILs[32, 40, 41] and the TMG-based ILs[13, 42, 43]. For example, Hong et al[41] developed the ether-functionalized imidazolium-based ILs as highly efficient SO_2 absorbents, which could exhibit very high capacity of up to 6.30 molSO_2·molIL^{-1} (0.74 gSO_2·gIL^{-1}) at 30℃ and 0.1 MPa. Subsequently, Wang et al[32] designed a new ether-functionalized IL with tetrazolate anion for SO_2 capture, and the absorption capacity could achieve as high as 5.00 molSO_2·molIL^{-1} (0.76 gSO_2·gIL^{-1}) at 20℃ and 0.1MPa through chemical and physical absorption. Based on the above discussion, it was proved that in fact the functional groups on the cation also have a very positive effect on SO_2 absorption besides the anions. Meanwhile, although these functionalized ILs have extremely high molar capacity of SO_2 absorption comparing with conventional ILs, their gravimetric capacity of SO_2 is still relatively low.

In our previous work[27], considering the advantages of pyridinium-based ILs such as high thermal stability, lower cost and higher biodegradability, a series of conventional pyridinium-based ILs were synthesized and used for SO_2 capture. It was found that [C_4Py][SCN] has very high gravimetric capacity of 0.84 gSO_2·gIL^{-1} under ambient

conditions, which is much higher than that of most reported functionalized ILs. As a successive work towards further exploring more highly efficient ILs for reversible capture of SO_2, a new method was developed by introducing different active sites, such as the tertiary amino group, the nitrile group and the ether group onto the cation of pyridinium-based ILs with the thiocyanate anion. In this study, three kinds of novel cation-functionalized ILs [NEt_2C_2Py][SCN], [C_4OPy][SCN] and [C_4CNPy][SCN] with high gravimetric capacity of SO_2 absorption were synthesized. The effect of different functionalized groups on their physicochemical properties and the performances of SO_2 absorption were systematically investigated. Meanwhile, the effect of different conditions (such as temperature, partial pressure of SO_2 and the water contents in ILs) on the absorption performances, SO_2/CO_2 selectivity and the regeneration and recyclability of ILs were also studied. Moreover, the role of the tertiary amino group, nitrile group and ether group in SO_2 capture was well explained through both the experiments (FT-IR and NMR spectroscopy) and Quantum Chemical calculations.

2. Results and discussion

2.1 Physicochemical properties

The physicochemical properties of four pyridinium-based ILs with the same anion [SCN] including the tertiary amino-functionalized IL [NEt_2C_2Py][SCN]), the ether-functionalized IL ([C_4OPy][SCN]), the nitrile-functionalized IL ([C_4CNPy][SCN]) and the conventional IL ([C_4Py][SCN]) were studied. Density and

viscosity of the ILs in this work as a function of the temperature were shown in Fig.S1 and Fig.S2, and the effect of different substituent groups on the pyridinium cation on their physical properties were studied. Clearly, the groups on the cation of pyridinium-based ILs have an obvious effect on the density and viscosities of ILs. As seen in Fig.S1, Comparing with the conventional IL $[C_4Py][SCN]$, two kinds of cation-functionalized ILs, such as $[C_4OPy][SCN]$ and $[C_4CNPy][SCN]$, showed the higher density due to the introduction of ether and nitrile groups on the pyridinium cation, while there was only a slight decrease in the density of the amino-functionalized IL $[NEt_2C_2Py][SCN]$, which was very close to that of $[C_4Py][SCN]$[27]. Similarly, as shown in Fig.S2, the grafting of a tertiary amino group and a nitrile group onto the cation notably leaded to an increase in viscosity, while the incorporation of an ether group could effectively decrease the viscosity. For example, the viscosities of $[NEt_2C_2Py][SCN]$ and $[C_4CNPy][SCN]$ were 612.43 and 313.46 mPa·s at 20℃, respectively, which exhibited higher viscosities than that of $[C_4Py][SCN]$ (107.34 mPa·s at 20℃) with only alkyl-based group on the cation. However, the viscosity of $[C_4OPy][SCN]$ as 94.07 mPa·s at 20℃ was obviously lower than the that of alkyl-substituted one, which showed the same viscosity reduction trend as that for other ether-functionalized ILs based on different cations[44, 45].

In addition, the effect of different substituent groups on thermal stability was also studied. As shown in Fig.S3, the thermal decomposition temperatures of $[NEt_2C_2Py][SCN]$, $[C_4OPy][SCN]$ and $[C_4CNPy][SCN]$ were 160□, 232□ and 228□,

respectively. Compared with the non-functionalized counterpart [C_4Py][SCN] (220□), the incorporation of ether group and nitrile group could improve slightly the thermal stability of [C_4OPy][SCN] and [C_4CNPy][SCN], while [NEt_2C_2Py][SCN] exhibited a relatively lower thermal stability, which may be mainly attributed to the increased basicity due to the presence of a tertiary amino group[31].

2.2 Effect of different cations on SO_2 absorption

Taking into account the high absorption capacity of SO_2 and excellent reversibility for the pyridinium-based IL [C_4Py][SCN] [27], therefore, the anion [SCN] was selected to pair with different cations containing a tertiary amino group, a nitrile group and an ether group on the pyridinium, and the effect of these groups on SO_2 capture was investigated. As shown in Fig.1, the tertiary amino-functionalized IL [NEt_2C_2Py][SCN] exhibited the highest absorption capacity of SO_2 among the investigated ILs, which can capture 3.958 molSO_2·molIL^{-1} at 20℃ and 0.1 MPa. Under the same conditions, the capacity of SO_2 absorption for [C_4OPy][SCN] and [C_4CNPy][SCN] could be as high as 2.956 and 2.917 molSO_2·molIL^{-1}, respectively, whereas the capacity in [C_4Py][SCN] was 2.553 molSO_2·molIL^{-1}. Obviously, the cation-functionalized ILs exhibited enhanced absorption of SO_2 in comparison with [C_4Py][SCN] containing non-functionalized group on the cation, indicating these functionalized groups on the cation have a positive impact on improving SO_2 capture.

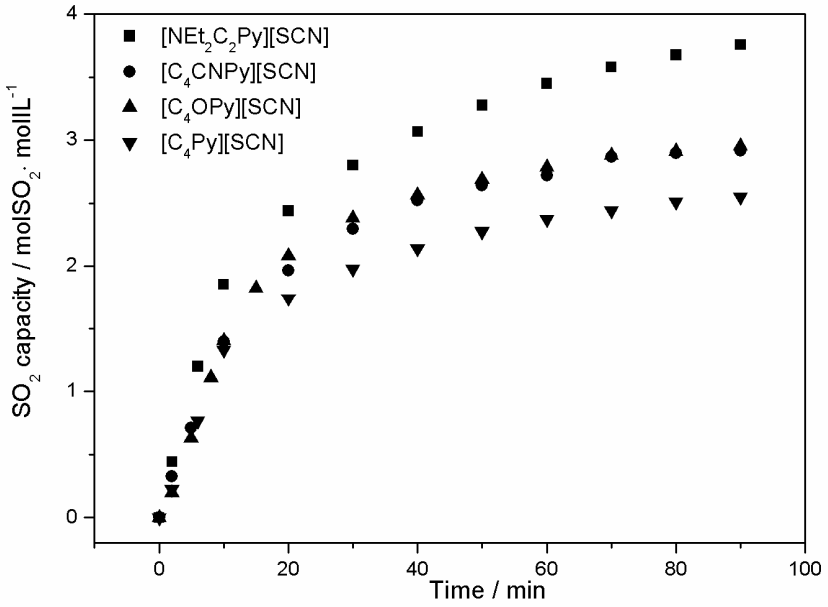

Fig.1 SO_2 absorption by cation-functionalized ILs at 20℃ and 0.1 MPa

2.2 Effect of temperature and pressure on SO_2 absorption

The effect of temperature and SO_2 partial pressure on SO_2 absorption by the cation-functionalized ILs were shown in Fig.2. As shown in Fig.2(a), the SO_2 absorption capacity of $[NEt_2C_2Py][SCN]$, $[C_4OPy][SCN]$ and $[C_4CNPy][SCN]$ at 0.1MPa decreased continuously as the temperature increased. For instance, the molar ratios of SO_2 to IL for $[NEt_2C_2Py][SCN]$, $[C_4CNPy][SCN]$ and $[C_4Py][SCN]$ decreased dramatically from 3.958, 2.917 and 2.553 to 1.411, 0.853 and 0.950 with an increase of temperature from 20 to 80℃, respectively. It was found that comparing with $[C_4Py][SCN]$ the temperature has more great influence on SO_2 absorption for $[C_4CNPy][SCN]$, which means that heating may be more favorable for SO_2 capture

by [C_4CNPy][SCN] to be released completely due to the introduction of the nitrile group into the cation.

The pressure dependence of SO_2 absorption by [NEt_2C_2Py][SCN], [C_4OPy][SCN] and [C_4CNPy][SCN] at 20□ was presented in Fig. 2(b). As expected, the SO_2 partial pressure also played a significant role in SO_2 absorption, and the SO_2 absorption capacity of [NEt_2C_2Py][SCN], [C_4CNPy][SCN] and [C_4Py][SCN] increased sharply with an increase of SO_2 partial pressure. For example, the molar ratios of SO_2 to [NEt_2C_2Py][SCN] and [C_4CNPy][SCN] increased from 1.363 to 3.958 and 0.652 to 2.917, respectively, when the SO_2 partial pressure changed from 0.01 to 0.1 MPa. Meanwhile, considering the low concentration of SO_2 in the real flue gas, the SO_2 absorption capacity for three kinds of cation-functionalized ILs at 5 kPa and 2 kPa of SO_2 partial pressure was also studied. The results showed that the absorption capacity of cation-functionalized ILs was less than 1 molSO_2·molIL^{-1} as the partial pressure of SO_2 was lower than 5 kPa. For instance, the molar ratio of SO_2 to [NEt_2C_2Py][SCN] was 0.807 at 5 kPa and 0.126 at 2kPa, respectively.

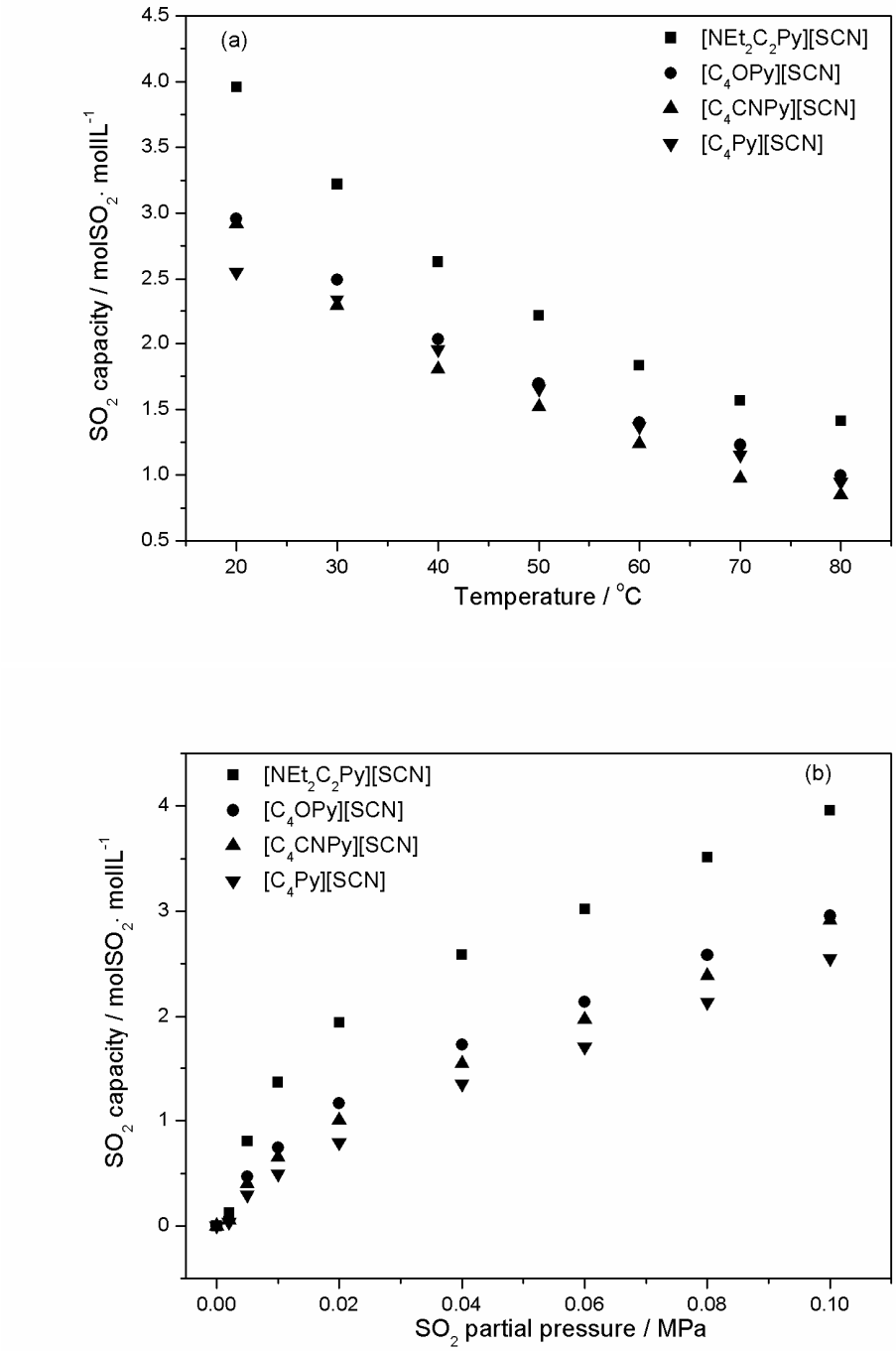

Fig.2 Effect of temperature at 0.1MPa (a) and SO_2 partial pressure at 20℃ (b) on SO_2 absorption by cation-functionalized ILs

2.3 SO_2/CO_2 Selectivity

As we know, there are usually other gases besides the low concentration of SO_2 in flue gas, such as CO_2, O_2 and N_2, so gas selectivity for judging the separation performance of a solvent becomes particularly important[11]. As reported by Brennecke et al[46] and our previous work[27], N_2 and O_2 solubility in ILs are generally much lower than CO_2 and SO_2 solubility, which suggests that the effective separation of two kinds of acid gases (SO_2 and CO_2) is the key procedure. Consequently, SO_2/CO_2 selectivity for $[NEt_2C_2Py][SCN]$, $[C_4OPy][SCN]$ and $[C_4CNPy][SCN]$ was studied and the results were listed in Table 1. Comparing with $[C_4Py][SCN]$, the remarkable improvement in SO_2/CO_2 selectivity for the three kinds of cation-functionalized ILs was achieved. Especially for $[C_4OPy][SCN]$ and $[C_4CNPy][SCN]$, SO_2/CO_2 selectivity substantially improved about 41% and 25%, respectively, which is more than 1.5 times that of $[P_{66614}][Tetz]$[30]. The nature may be that the increase of the ILs' polarity induced by an ether group and a nitrile group resulted in the enhanced absorption of polar SO_2 gas and slightly decreased absorption of non-polar CO_2 gas[44, 47, 48].

Table 1 SO_2/CO_2 selectivity for cation-functionalized ILs (20℃, 0.1 MPa)

ILs	molgas·molIL^{-1}		Selectivity
	SO_2	CO_2	SO_2/CO_2
$[NEt_2C_2Py][SCN]$	3.958	0.061	65
$[C_4CNPy][SCN]$	2.917	0.037	79
$[C_4OPy][SCN]$	2.956	0.042	70
$[C_4Py][SCN]$[27]	2.553	0.045	56

2.4 Effect of H_2O on SO_2 absorption

In practical applications, water is always accompanied with SO_2 in flue gas, and during SO_2 absorption the water can be also absorbed into absorbents. Therefore, the effect of water on SO_2 absorption by $[NEt_2C_2Py][SCN]$, $[C_4CNPy][SCN]$ and $[C_4OPy][SCN]$ was investigated at 20℃ and 0.1 MPa and the results were shown in Fig.3 and Fig.S4, respectively. It was demonstrated that the presence of water has a different impact on SO_2 absorption for the three kinds of cation-functionalized ILs. For $[C_4CNPy][SCN]$ (Fig.3(a)) and $[C_4OPy][SCN]$ (Fig.S4), SO_2 absorption capacity in the two ILs decreased slightly with an increase of water content, while SO_2 absorption capacity in $[NEt_2C_2Py][SCN]$ (Fig.3(b)) increased a little after the addition of water. For example, when the water in ILs increased to about 1.0%, the molar ratio of SO_2 to $[C_4CNPy][SCN]$ decreased from 2.917 to 2.851, while SO_2 absorption capacity in $[NEt_2C_2Py][SCN]$ increased from 3.958 to 4.181 $molSO_2 \cdot molIL^{-1}$. The results indicated that the water present in $[C_4CNPy][SCN]$ and $[C_4OPy][SCN]$ plays a negative role in SO_2 absorption capacity, but is favorable for improving SO_2 absorption capacity in $[NEt_2C_2Py][SCN]$. The detail reason will be discussed in the section of the mechanism.

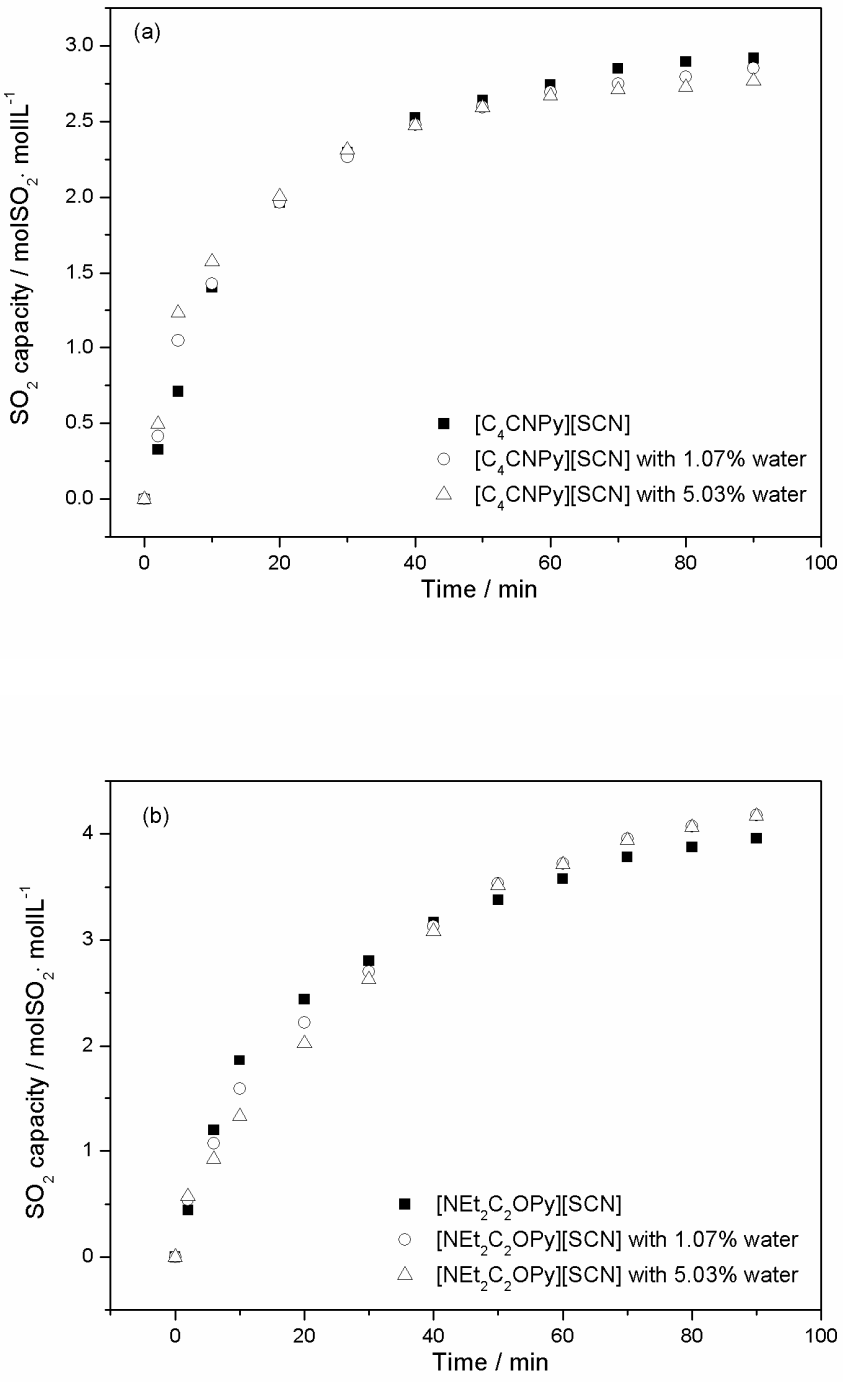

Fig.3 Effect of water on SO_2 absorption capacity by $[C_4CNPy][SCN]$ (a) and $[NEt_2C_2Py][SCN]$ (b) at 20℃ and 0.1 MPa

2.5 Regeneration and recycle of ionic liquids

In order to examine the reversibility of SO_2 absorption, multiple consecutive cycles of SO_2 absorption and desorption for $[NEt_2C_2Py][SCN]$, $[C_4OPy][SCN]$ and $[C_4CNPy][SCN]$ were studied. As shown in Fig.4, SO_2 captured by the three types of cation-functionalized ILs could be almost completely stripped out at 80□ by bubbling N_2 through the ILs for 60 min, which was further proved by FT-IR spectra of $[NEt_2C_2Py][SCN]$ (Fig.5), $[C_4CNPy][SCN]$ (Fig.6) and $[C_4OPy][SCN]$ (Fig.S5) before absorption and after desorption of SO_2. Comparing with $[C_4Py][SCN]$, the residual capacity of SO_2 absorption by $[C_4CNPy][SCN]$ decreased from 0.099 to 0.055 $molSO_2 \cdot molIL^{-1}$, implying that the desorption of SO_2 is enhanced owing to the presence of the nitrile group, which agrees well with the former results. Meanwhile, these cation-functionalized ILs can be repeatedly used and still remain the stable absorption performances after five cycles of absorption and desorption, which indicated that the process of SO_2 absorption and desorption by these cation-functionalized ILs is highly reversible and the ILs are recyclable.

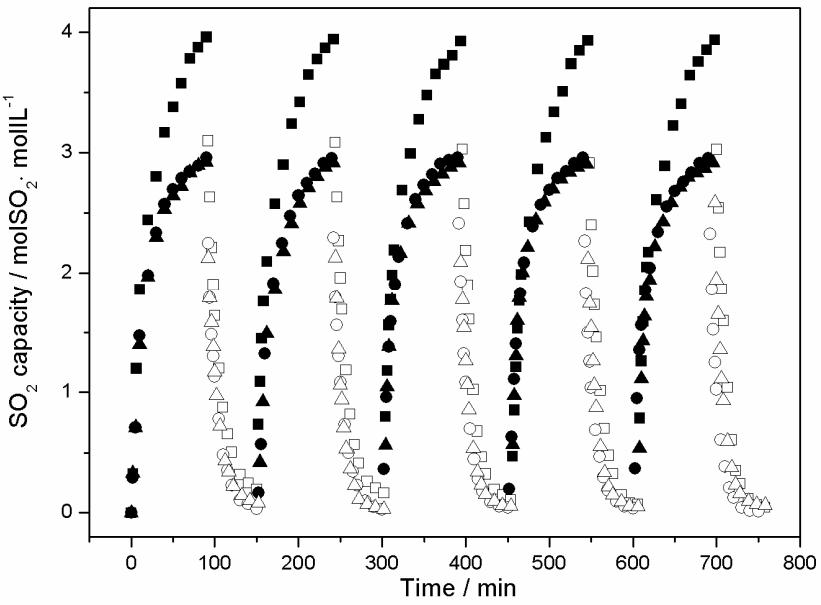

Fig.4 SO_2 absorption and desorption by cation-functionalized ILs. SO_2 absorption was carried out at 20℃, and SO_2 desorption at 80℃ under N_2. $[NE_2tC_2Py][SCN]$, absorption ■, desorption □; $[C_4OPy][SCN]$, absorption ●, desorption ○; $[C_4CNPy][SCN]$, absorption ▲, desorption Δ.

2.6 Comparison with other ionic liquids

To our knowledge, the mass of SO_2 absorbed per unit mass of IL is of great importance in industrial separation processes[11, 33]. Therefore, in order to evaluate the potential of ILs for SO_2 capture, gravimetric absorption capacity of SO_2 for the three types of cation-functionalized ILs was compared with other ILs reported in literature in Table 2. It was clearly seen that although the molar absorption capacity of SO_2 in the investigated cation-functionalized ILs is slightly lower than some reported functionalized ILs, their corresponding gravimetric capacity of SO_2 is very high. Especially the tertiary amino-functionalized IL $[NEt_2C_2Py][SCN]$ exhibited the

highest absorption capacity of 1.06 $gSO_2 \cdot gIL^{-1}$ under atmospheric pressure in this work, which is very close to the maximum value (1.13 $gSO_2 \cdot gIL^{-1}$) reported to date[49], and even could absorb as high as 0.37 $gSO_2 \cdot gIL^{-1}$ under low SO_2 partial pressure of 0.01MPa. The results indicated the pyridinium-based IL $[NEt_2C_2Py][SCN]$ will be a good candidate for SO_2 removal from flue gases.

Table 2 Comparison of SO_2 absorption capacity with other ILs

ILs	Temperature	SO_2 absorption [a]		Selectivity	References
	℃	0.1MPa	0.01MPa	SO_2/CO_2	
$[NEt_2C_2Py][SCN]$	20	1.06 (3.958)	0.37 (1.411)	65	This work
$[C_4OPy][SCN]$	20	0.90 (2.956)	0.23 (0.950)	70	This work
$[C_4CNPy][SCN]$	20	0.85 (2.917)	0.20 (0.853)	79	This work
$[C_4Py][SCN]$	20	0.84 (2.55)	0.16 (0.49)	56	[27]
[Emim][SCN]	20	1.13 (2.99)	0.37 (0.98)	-	[49]
$[P_{66614}][SCN]$	20	0.38 (3.24)	0.13 (1.06)	-	[49]
$[P_{66614}][BenIm]$	20	0.61(5.75)	0.26 (2.59)	-	[31]
$[P_{66614}][Tetz]$	20	0.43 (3.72)	0.18 (1.54)	47	[30]
$[P_{66614}][4\text{-Br-phCOO}]$	20	0.38 (4.12)	0.15 (1.66)	-	[34]
$[P_{444E3}][Tetz]$	20	0.76 (5.00)	0.29 (1.87)	-	[32]
$[E_3mim][Tetz]$	20	0.95 (4.43)	0.34 (1.58)	-	[32]
$[E_8mim][MeSO_3]$	30	0.74 (6.30)	-	-	[41]
[Bmim][OAc]	20	0.62 (1.91)	0.21(0.66)	-	[38]
[TMG]L	40	0.53 (1.70)	0.31(0.98)	-	[42]
$[TMG][BF_4]$	20	0.40 (1.27)	0.02 (0.06)	-	[17]

[a] $gSO_2 \cdot gIL^{-1}$ ($molSO_2 \cdot molIL^{-1}$)

2.7 The mechanism for SO_2 absorption

In order to understand the role of the different substituent groups on the cation in SO_2 absorption, FTIR and NMR spectroscopy were used to investigate the interaction between ILs and SO_2. The FT-IR spectra of fresh ILs, SO_2-absorbed ILs and ILs after desorption for $[NEt_2C_2Py][SCN]$, $[C_4CNPy][SCN]$ and $[C_4OPy][SCN]$ were shown in Fig.5, Fig.6 and Fig.S5, respectively. As shown in Fig.5, compared with the FTIR spectrum of the fresh IL $[NEt_2C_2Py][SCN]$, three new absorption bands centered at 1315, 1132 and 946 cm^{-1} were observed in the FTIR spectrum of $[NEt_2C_2Py][SCN]$ after uptake of SO_2. The peaks appearing at 1315 and 1132 cm^{-1} could be assigned to the asymmetric and symmetric S=O stretches, and another new peak at 946 cm^{-1} was attributed to the formation of S-O bonds as a result of SO_2 absorption, which indicated the chemical interaction exists between the amino-functionalized IL $[NEt_2C_2Py][SCN]$ and SO_2 by the formation of a charge transfer complex[50, 51] besides the physical interaction between the anion [SCN] and SO_2[30-32].

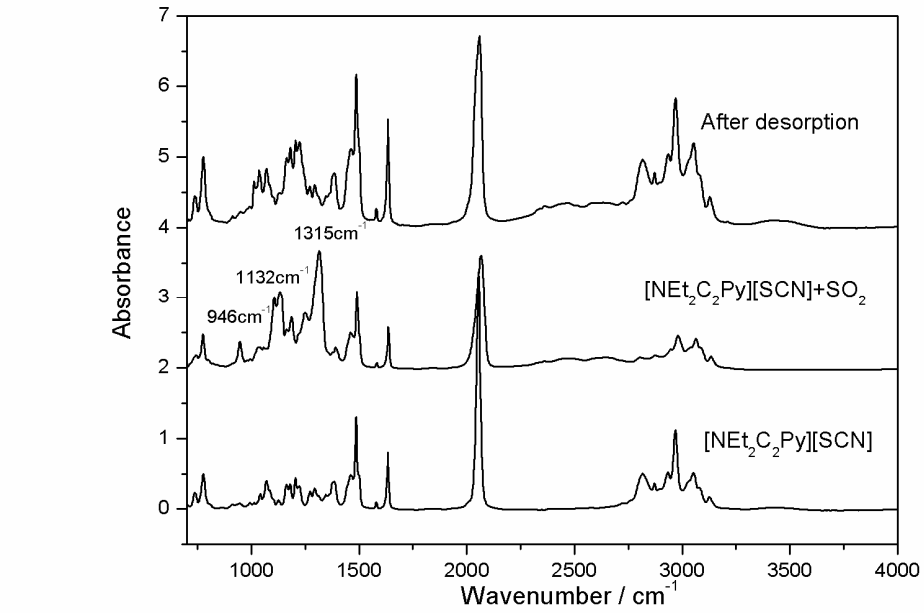

Fig.5 FT-IR spectra of $[NEt_2C_2Py][SCN]$ before and after SO_2 absorption and after SO_2 desorption

For the nitrile-functionalized IL $[C_4CNPy][SCN]$, there were only two new bands at 1296 and 1124 cm^{-1} for the asymmetric and symmetric S=O stretches in the FTIR spectrum of $[C_4CNPy][SCN]$ saturated with SO_2 gas (Fig.6), which indicated that only physical absorption of SO_2 occurs in the nitrile-functionalized IL $[C_4CNPy][SCN]$. Similarly, the changes in the spectra of the ether-functionalized IL $[C_4OPy][SCN]$ before and after SO_2 absorption showed the same results (Fig.S5), which is consistent with those previously reported by Hong et al[41] and Wang et al[32].

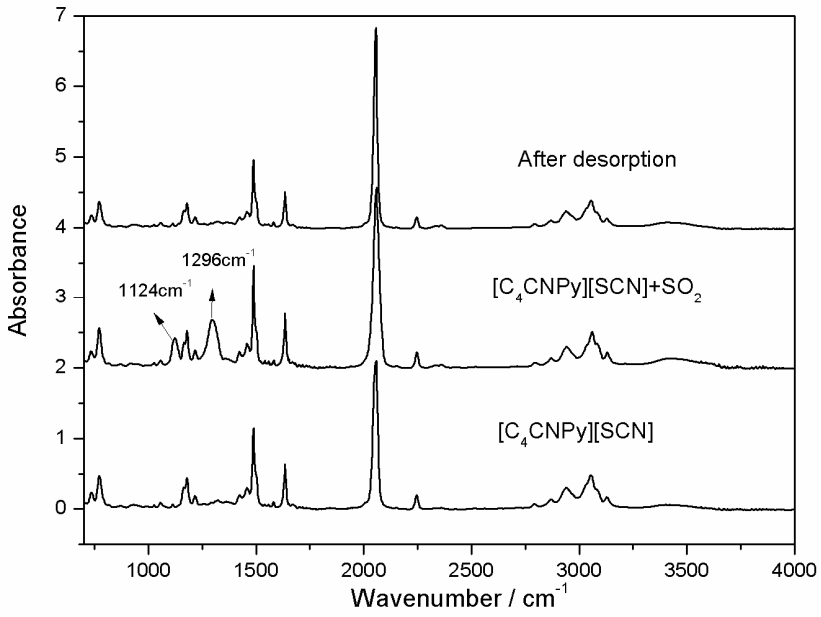

Fig.6 FT-IR spectra of $[C_4CNPy][SCN]$ before and after SO_2 absorption and after SO_2 desorption

Furthermore, the FT-IR spectra of fresh ILs, SO_2-absorbed ILs and ILs after desorption for $[NEt_2C_2Py][SCN]$, $[C_4CNPy][SCN]$ and $[C_4OPy][SCN]$ with water were shown in Fig.7, Fig.8 and Fig.S6, respectively. Compared with FT-IR spectra of $[NEt_2C_2Py][SCN]$ without water after SO_2 absorption, a new peak at 1034 cm^{-1} corresponding to S-OH were observed in FT-IR spectrum of $[NEt_2C_2Py][SCN]$ with water after SO_2 absorption (Fig.7), which indicated that the enhanced absorption of SO_2 for $[NEt_2C_2Py][SCN]$ in the presence of water could be ascribed to the formation of hydrogen sulfite salts. The results showed good agreements with that reported by Sayari et al[4, 5, 52, 53]. As shown in Fig.8 and Fig.S6, the results indicated that the presence of water does not change the physical absorption process between $[C_4CNPy][SCN]$/$[C_4OPy][SCN]$ and SO_2, and the structure of

$[C_4CNPy][SCN]/[C_4OPy][SCN]$ with water after absorption and desorption of SO_2 can also keep stable.

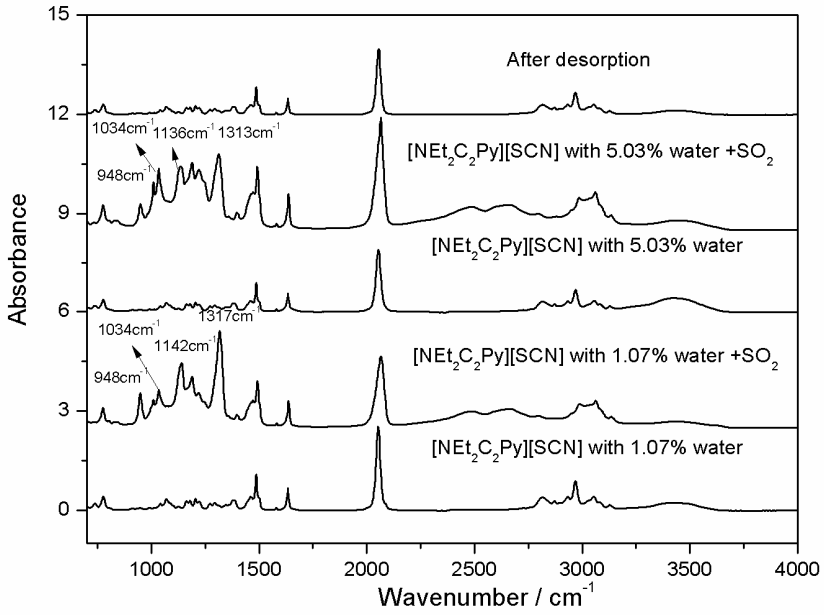

Fig.7 FT-IR spectra of $[NEt_2C_2Py][SCN]$ with water before and after absorption of SO_2 and after desorption

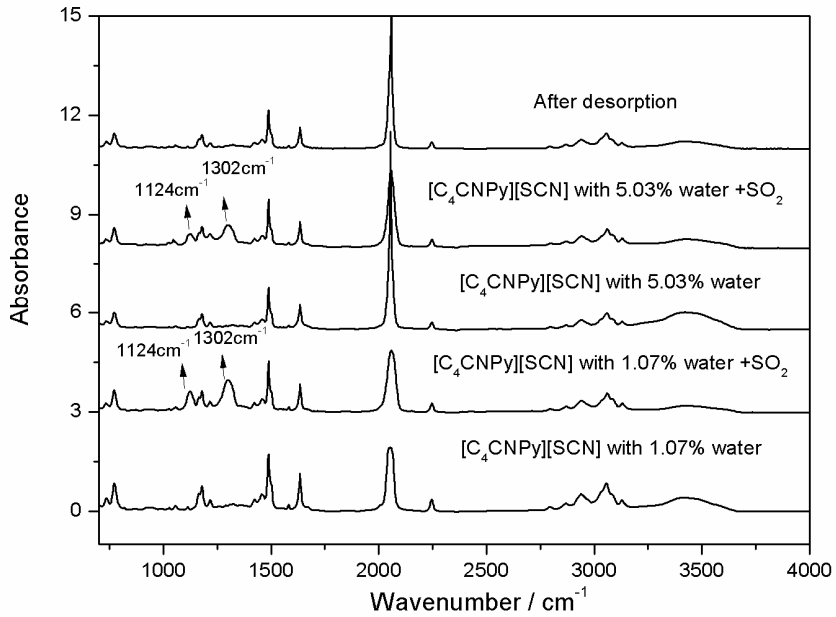

Fig.8 FT-IR spectra of $[C_4CNPy][SCN]$ with water before and after absorption of SO_2 and after desorption

The ^1H NMR and ^{13}C NMR spectra of $[NEt_2C_2Py][SCN]$, $[C_4CNPy][SCN]$ and $[C_4OPy][SCN]$ before and after SO_2 absorption were further compared in Fig.9, Fig.10 and Fig.S7, respectively. As shown in Fig.9, after the absorption of SO_2, typical peaks in the ^1H NMR spectrum of the cation in $[NEt_2C_2Py][SCN]$ moved downfield from 2.44 and 2.86 ppm to 2.58 and 2.99 ppm, respectively. Meanwhile, the corresponding ^{13}C NMR signals showed upfield shifting from 53.01 and 59.52 ppm to 52.53 and 58.72 ppm, respectively. These chemical shifts further proved that there exists the chemical interaction between the tertiary amino group on the pyridinium ring and SO_2. Additionally, neither new peaks or significant chemical shifts were observed after SO_2 absorption by the nitrile-functionalized IL

[C_4CNPy][SCN] (Fig.10) and ether-functionalized IL [C_4OPy][SCN] (Fig.S7), which agrees well with the IR results.

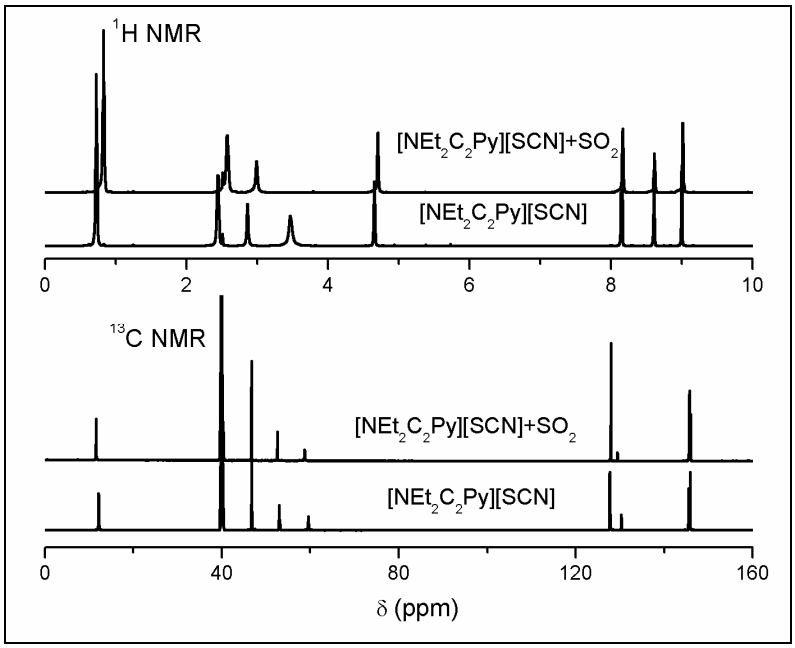

Fig.9 ^{1}H NMR and ^{13}C NMR spectra of [NEt_2C_2Py][SCN] before and after SO_2 absorption

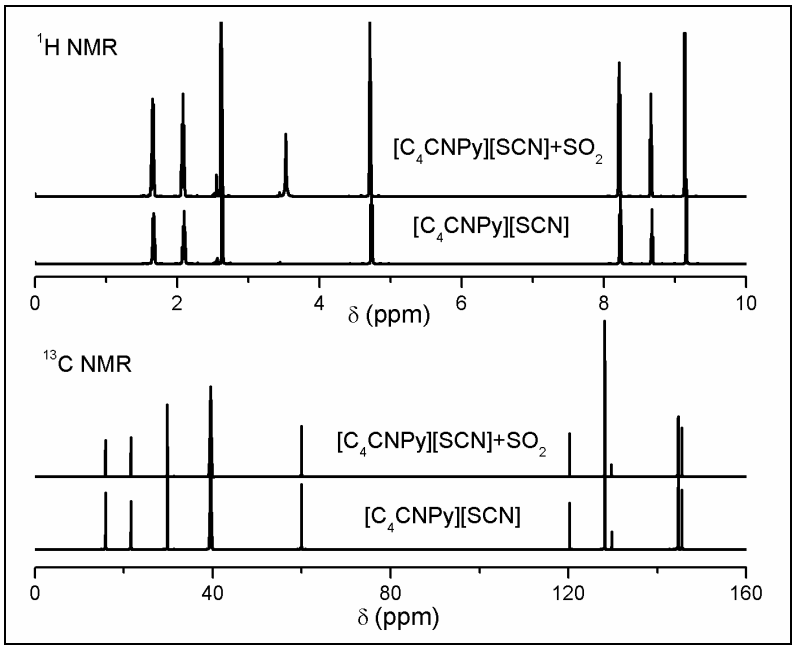

Fig.10 ^{1}H NMR and ^{13}C NMR spectra of [C_4CNPy][SCN] before and after SO_2 absorption

Moreover, the density functional theory calculations were performed using Gaussian 09 program to further investigate the interaction between ILs and SO_2. The optimized structures of IL-SO_2 systems for [NEt_2C_2Py][SCN], [C_4OPy][SCN], [C_4CNPy][SCN] and [C_4Py][SCN] were presented in Fig.11. As shown in Fig.11(a), 11(b) and 11(c), the interactions between SO_2 and these three pyridinium-based ILs are very different. Compared with that of [C_4Py][SCN]-SO_2, the intermolecular distance between the sulfur atom of SO_2 and the sulfur atom of SCN anion in [C_4OPy][SCN]-SO_2 and [C_4CNPy][SCN]-SO_2 became slightly shorter. Meanwhile, three hydrogen bonds formed between SO_2 molecule and the cations of [C_4CNPy][SCN] and [C_4OPy][SCN] whereas only two hydrogen bonds formed between SO_2 molecule and the cation of [C_4Py][SCN], suggesting the stronger interaction between SO_2 and [C_4OPy][SCN] or [C_4CNPy][SCN]. The results may further prove the higher absorption capacity of SO_2 using [C_4OPy][SCN] and [C_4CNPy][SCN] than [C_4Py][SCN], which is consistent with the experimental results. However, for [NEt_2C_2Py][SCN] that physically and chemically absorb SO_2, the optimized structures of IL-SO_2 in Fig.11(d) showed that the physical interaction of [NEt_2C_2Py][SCN] with SO_2 was almost similar to that of [C_4Py][SCN]-SO_2. Therefore, it was reasonably believed that the enhancement in SO_2 absorption for [NEt_2C_2Py][SCN] mainly originated from the strong chemical interaction between the tertiary amino group and SO_2.

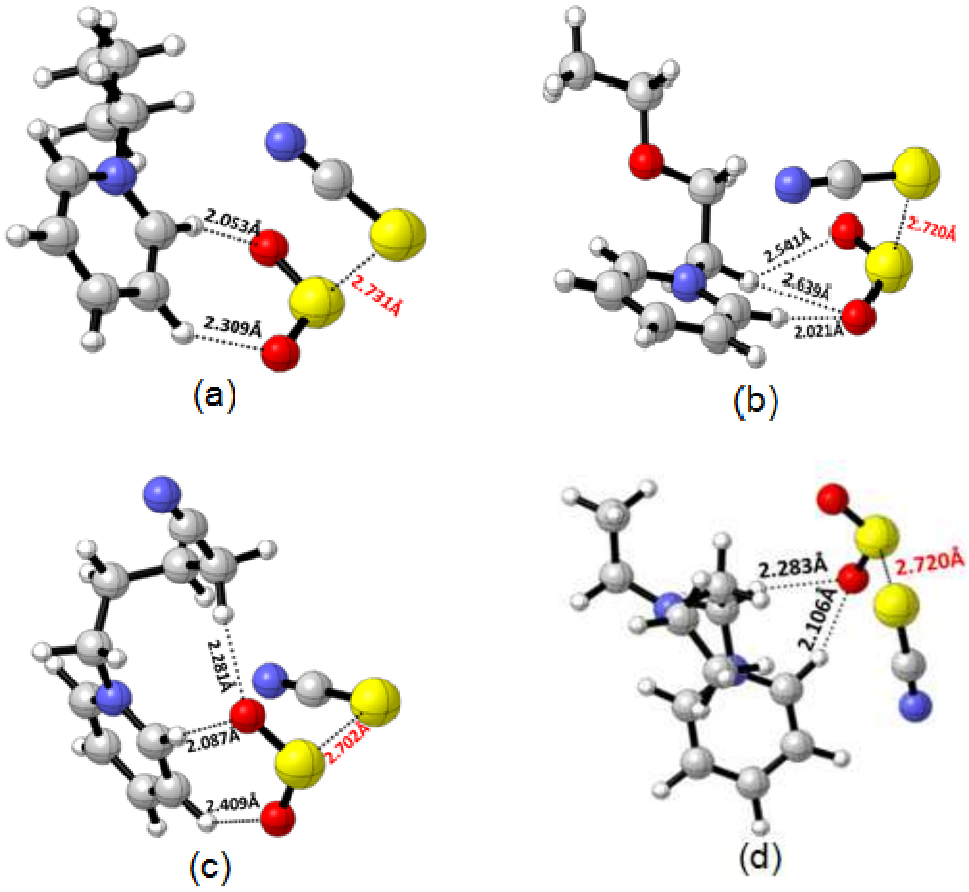

Fig.11 Optimized structures showing the interactions of ILs with SO_2 molecules: (a) $[C_4Py][SCN]$-SO_2 (ΔH= -67.3 kJ·mol^{-1}), (b) $[C_4OPy][SCN]$-SO_2(ΔH= -68.8 kJ·mol^{-1}), (c) $[C_4CNPy][SCN]$-SO_2 (ΔH= -62.8 kJ·mol^{-1}), (d) $[NEt_2C_2Py][SCN]$-SO_2 (ΔH= -63.9 kJ·mol^{-1}). H: light gray, C: gray, O: red, N: blue, S: yellow

In addition, the interaction enthalpies ΔH between ILs and SO_2 were calculated as -67.3, -68.8, 63.9 and -62.8 kJ·mol^{-1} for $[C_4Py][SCN]$, $[C_4OPy][SCN]$, $[NEt_2C_2Py][SCN]$ and $[C_4CNPy][SCN]$, respectively. It is clearly observed that ΔH of $[C_4OPy][SCN]$-SO_2 is comparable to that of $[C_4Py][SCN]$-SO_2, however, ΔH of $[NEt_2C_2Py][SCN]$-SO_2 and $[C_4CNPy][SCN]$-SO_2 is slightly lower than that of $[C_4Py][SCN]$-SO_2, which means that the cation-functionalized ILs may be more

efficient for SO_2 absorption due to their higher SO_2 absorption capacity and comparable or lower interaction enthalpies.

3. Experimental

3.1 Materials

SO_2 gas (99.9%) was supplied by Beijing Beiwen Gas Factory. N, N-diethyl-2-amino-1-bromoethane hydrobromide (98%), 2-chloroethyl ethyl ether (98%), and 5-Chlorovaleronitrile (97%) were purchased from TCI. Other chemical reagents of analytical grade, including pyridine, 1-bromobutane, ethyl acetate, dichloromethane, acetone, ethanol, acetonitrile, methanol, diethyl ether and sodium thiocyanate were purchased from Beijing Chemical Company. All reagents were used for the synthesis of the ILs without further purification.

3.2 Synthesis and characterizations of ILs

Three types of cation-functionalized ILs with the same anion [SCN] including 1-(2-diethylaminoethyl)pyridinium thiocyanate ($[NEt_2C_2Py][SCN]$), 1-ethyoxylethylpyridinium thiocyanate ($[C_4OPy][SCN]$) and 1-valeronitrilepyridinium thiocyanate ($[C_4CNPy][SCN]$) were synthesized in a two-step method, and the preparations of ILs were shown below. The structures of the ILs studied in this work were shown in Fig.12.

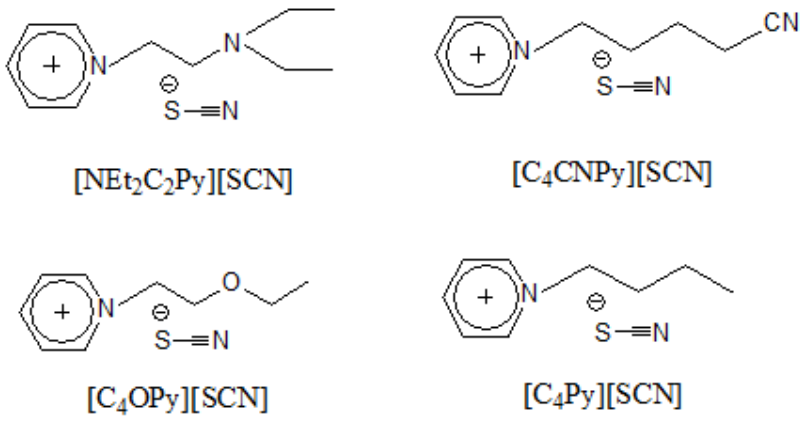

Fig.12 Structures of pyridinium-based ILs with different groups on the cation

Synthesis of $[NEt_2C_2Py][SCN]$: The IL $[NEt_2C_2Py][SCN]$ was synthesized following the preparation procedures of 1-(N,N-dimethylaminoethyl)-2,3-dimethylimidazolium trifluoro-methanesulfonate ([mammim][TfO])[54]. In the experiment, pyridine (7.62 g, 0.096 mol) and N,N-diethyl-2-amino-1-bromoethane hydrobromide (25.15 g, 0.096 mol) were dissolved in acetonitrile (200 mL) and heated under reflux at 80℃ for 48 h. After cooling to room temperature, the mixture was filtered and the remaining solid was washed with acetone (3×40 ml). After drying at 60℃ under vacuum for 48 h, $[NEt_2C_2Py][Br][HBr]$ was obtained as white solid. $[NEt_2C_2Py][Br][HBr]$ (29.65 g, 0.087 mol) and NaOH (3.49 g, 0.087 mol) were added in methanol (25 mL) at 0-5℃ and stirred for 12 h at room temperature. Then equimolar NaSCN (7.069g, 0.087mol) was added and stirred for 24 h. After that time the methanol was removed by rotary evaporation, and the mixtures were washed with dichloromethane (200 ml). After filtration and removal of solvents from filtrate, the yellowish oil $[NEt_2C_2Py][SCN]$ was finally obtained under vacuum at 50℃ for 48 h.

Synthesis of $[C_4CNPy][SCN]$: Pyridine (10.614 g, 0.134 mol) and

5-Chlorovaleronitrile ($Cl(CH_2)_4CN$, 15.778 g, 0.134 mol) were firstly mixed and stirred at 80℃ for 8 h, then the reaction mixture was stirred at 110℃ for 40 h. After cooling to room temperature, the reaction mixture was washed with diethyl ether (3×40 ml) and dried at 80℃ under vacuum for 48 h to obtain the pale yellow solid $[C_4CNPy]Cl$. The anion exchange reaction was performed by mixing $[C_4CNPy]Cl$ (28.706 g, 0.146 mol) and equimolar NaSCN in acetone (200 ml). After stirring for 48 h at room temperature, the mixture was filtered and washed with acetone (3×100 ml). The organic layer was collected and concentrated by rotary evaporation to remove the solvent. The product $[C_4CNPy][SCN]$ was finally obtained as the dark orange liquid under vacuum at 50℃ for 48 h.

Synthesis of $[C_4OPy][SCN]$: 2-Chloroethyl ethyl ether (20.524 g, 0.185 mol) was added to pyridine (14.654 g, 0.185 mol) while stirring at 100℃ for 48 h. After the reaction, ethanol (150 mL) and activated carbon (8 g) were added into the reaction solution at room temperature, and the mixture kept stirring for 3 h. After filtration and removal of the solvents by rotary evaporation, the resulting product was washed with ethyl acetate (3×40 ml), and dried under vacuum at 75℃ for 48 h to afford $[C_4OPy]Cl$ as the brown solid. The IL $[C_4OPy][SCN]$ was synthesized following the same procedures described above for $[C_4CNPy][SCN]$, except for the use of $[C_4OPy]Cl$ instead of $[C_4CNPy]Cl$. The final product $[C_4OPy][SCN]$ was obtained as the brown liquid under vacuum at 50℃ for 48 h.

All the ILs were dried under vacuum at 50℃ for 48 h before use. The structures of these ILs were confirmed by ^1H and ^{13}C NMR spectroscopy with Bruker 600

spectrometer and FT-IR spectroscopy by a Thermo Nicolet 380 Spectrometer. The water content in the ILs after drying were determined with volumetric Karl Fischer Titration (Metrohm, 787 KF Titrino) and found to be less than 0.1wt%. The residual halide contents in the ILs were measured using PXSJ-226 Series Ion meter (INESA Scientific Instrument Co. Ltd), and found to be less than 0.3 wt%. Decomposition temperature was measured with a Thermogravimeric Analysis (TGA) 2050 meter. Densities and viscosities were measured on Paar DMA 5000 density and Paar AMVN viscosity meters, respectively.

3.3 Absorption and desorption of SO_2

The experiments for SO_2 absorption and desorption followed the same procedures of our previous work[27]. In a typical absorption of SO_2, the pure SO_2 was bubbled through about 5 g IL in the glass container with an inner diameter of 3.0 cm and a height of 12.0 cm at a flow rate of 140 ml min^{-1}. The temperature of the glass container was controlled at the desired temperature within ± 0.1℃ by a circulated water bath. The amount of SO_2 absorbed in the IL was measured using an electronic balance with an accuracy of ± 0.1mg and was finally determined according to the increase of the weight. For the absorption of SO_2 under reduced pressure, the gases of different SO_2 partial pressure were obtained by changing the flow of SO_2 and N_2.

SO_2 desorption from saturated IL solutions was carried out in a similar way to the absorption method mentioned above. The pure N_2 with the same flow rate was bubbled through the IL that absorbed SO_2 in the glass container at 80℃, the amount

of SO_2 desorption was determined at regular intervals by an electronic balance until the weight kept unchanged. The reproducibility of the absorption and desorption experiments was less than ± 3%, and it was estimated that the experimental error involved in the method was at the level of ± 5%.

4. Conclusions

In this work, three kinds of novel cation-functionalized ILs $[NEt_2C_2Py][SCN]$, $[C_4OPy][SCN]$ and $[C_4CNPy][SCN]$ were synthesized, and the effect of different functional groups on their physicochemical properties and the performances of SO_2 absorption were systematically investigated. The results demonstrated that these cation-functionalized ILs exhibited much better absorption capacity and SO_2/CO_2 selectivity than the conventional IL $[C_4Py][SCN]$. Among the investigated ILs, $[NEt_2C_2Py][SCN]$ exhibited the highest absorption capacity of 1.06 $gSO_2 \cdot gIL^{-1}$ under ambient conditions. Meanwhile, SO_2/CO_2 selectivity was greatly improved up to 41% through the incorporation of these groups on the cation of ILs. The present of water causes a slight decrease in SO_2 capacity by $[C_4CNPy][SCN]$ and $[C_4OPy][SCN]$, whereas a slight increase in SO_2 capacity by $[NEt_2C_2Py][SCN]$. Moreover, spectroscopic characterizations and Quantum Chemical calculation results indicated that only physical absorption of SO_2 occurs in $[C_4CNPy][SCN]$ and $[C_4OPy][SCN]$, but a combination of the chemical and physical interaction coexists between $[NEt_2C_2Py][SCN]$ and SO_2. The great enhancement in SO_2 absorption by $[NEt_2C_2Py][SCN]$ mainly originates from the strong chemical interaction between the

tertiary amino group and SO_2 besides the physical interaction of [SCN]-SO_2. In addition, the three kinds of cation-functionalized ILs could also keep the stable absorption performance after five cycles of absorption and desorption, implying these ILs show great potentials for the applications of SO_2 capture.

Acknowledgements

This work was supported by the key program of Beijing Municipal Natural Science Foundation (NO.2141003), the key program of the National Natural Science Foundation of China (NO.21436010), the External Cooperation Program of BIC, Chinese Academy of Sciences (No.GJHZ201301) and the National High Technology Research and Development Program of China (No.2013AA06540201).

Notes and references

[a] Beijing Key Laboratory of Ionic Liquids Clean Process, Key Laboratory of Green Process and Engineering, State Key Laboratory of Multiphase Complex Systems, Institute of Process Engineering, Chinese Academy of Sciences, Beijing, 100190, China

[b] College of Chemical and Engineering, University of Chinese Academy of Sciences, Beijing 100049, China

Email: sjzhang@home.ipe.ac.cn； xpzhang@home.ipe.ac.cn

Electronic Supplementary Information (ESI) available: NMR data, FTIR and NMR spectra of the investigated ILs before and after SO_2 abosprion, Densities and viscosities at different temperatures and TGA results of the ILs, and the effect of water on SO_2 absorption for [C_4OPy][SCN].

1. X. X. Ma, T. Kaneko, T. Tashimo, T. Yoshida and K. Kato, *Chem Eng Sci*, 2000, **55**, 4643-4652.
2. M. J. Renedo and J. Fernandez, *Ind Eng Chem Res*, 2002, **41**, 2412-2417.
3. F. J. G. Ortiz, F. Vidal, P. Ollero, L. Salvador, V. Cortes and A. Gimenez, *Ind Eng Chem*

Res, 2006, **45**, 1466-1477.
4. R. Tailor, A. Ahmadalinezhad and A. Sayari, *Chem Eng J*, 2014, **240**, 462-468.
5. R. Tailor, M. Abboud and A. Sayari, *Environ Sci Technol*, 2014, **48**, 2025-2034.
6. I. J. Uyanga and R. O. Idem, *Ind Eng Chem Res*, 2007, **46**, 2558-2566.
7. P. Bollini, S. A. Didas and C. W. Jones, *J Mater Chem*, 2011, **21**, 15100-15120.
8. D. Camper, J. E. Bara, D. L. Gin and R. D. Noble, *Ind Eng Chem Res*, 2008, **47**, 8496-8498.
9. C. Wang, H. Luo, D.-e. Jiang, H. Li and S. Dai, *Angew Chem Int Ed*, 2010, **49**, 5978-5981.
10. C. Wang, H. Luo, X. Luo, H. Li and S. Dai, *Green Chem*, 2010, **12**, 2019-2023.
11. M. Ramdin, T. W. de Loos and T. J. H. Vlugt, *Ind Eng Chem Res*, 2012, **51**, 8149-8177.
12. M. B. Shiflett, A. M. S. Niehaus, B. A. Elliott and A. Yokozeki, *Int J Thermophys*, 2012, **33**, 412-436.
13. S. Ren, Y. Hou, S. Tian, X. Chen and W. Wu, *The Journal of Physical Chemistry B*, 2013, **117**, 2482-2486.
14. J. Zhang, C. Jia, H. Dong, J. Wang, X. Zhang and S. Zhang, *Ind Eng Chem Res*, 2013, **52**, 5835-5841.
15. Y. Zhang, S. Zhang, X. Lu, Q. Zhou, W. Fan and X. Zhang, *Chem-Eur J*, 2009, **15**, 3003-3011.
16. J. L. Anderson, J. K. Dixon, E. J. Maginn and J. F. Brennecke, *J Phys Chem B*, 2006, **110**, 15059-15062.
17. J. Huang, A. Riisager, P. Wasserscheid and R. Fehrmann, *Chem Commun*, 2006, 4027-4029.
18. X. L. Yuan, S. J. Zhang and X. M. Lu, *J Chem Eng Data*, 2007, **52**, 1150-1150.
19. L. E. Barrosse-Antlle, C. Hardacre and R. G. Compton, *J Phys Chem B*, 2009, **113**, 1007-1011.
20. M. B. Shiflett and A. Yokozeki, *Ind Eng Chem Res*, 2010, **49**, 1370-1377.
21. G. Yu and X. Chen, *J Phys Chem B*, 2011, **115**, 3466-3477.
22. S. Ren, Y. Hou, W. Wu, Q. Liu, Y. Xiao and X. Chen, *J Phys Chem B*, 2010, **114**, 2175-2179.
23. G. Qu, J. Zhang, J. Li and P. Ning, *Separ Sci Technol*, 2013, **48**, 2876-2879.
24. J. Dupont, R. F. de Souza and P. A. Z. Suarez, *Chem Rev*, 2002, **102**, 3667-3691.
25. X. Zhang, X. Zhang, H. Dong, Z. Zhao, S. Zhang and Y. Huang, *Energy & Environmental Science*, 2012, **5**, 6668-6681.
26. S. Zhang, X. Zhang, Y. Zhao, G. Zhao, X. Yao and H. Yao, *Science China-Chemistry*, 2010, **53**, 1549-1553.
27. S. Zeng, H. Gao, X. Zhang, H. Dong, X. Zhang and S. Zhang, *Chem Eng J*, 2014, **251**, 248-256.
28. J. L. Anthony, J. L. Anderson, E. J. Maginn and J. F. Brennecke, *J Phys Chem B*, 2005, **109**, 6366-6374.
29. K. Y. Lee, C. S. Kim, H. Kim, M. Cheong, D. K. Mukherjee and K.-D. Jung, *B Kor Chem Soc*, 2010, **31**, 1937-1940.
30. C. Wang, G. Cui, X. Luo, Y. Xu, H. Li and S. Dai, *J Am Chem Soc*, 2011, **133**, 11916-11919.

31. G. Cui, W. Lin, F. Ding, X. Luo, X. He, H. Li and C. Wang, *Green Chem*, 2014, **16**, 1211.
32. G. Cui, C. Wang, J. Zheng, Y. Guo, X. Luo and H. Li, *Chem Commun*, 2012, **48**, 2633-2635.
33. D. Yang, M. Hou, H. Ning, J. Ma, X. Kang, J. Zhang and B. Han, *ChemSusChem*, 2013, **6**, 1191-1195.
34. G. Cui, J. Zheng, X. Luo, W. Lin, F. Ding, H. Li and C. Wang, *Angewandte Chemie International Edition*, 2013, **52**, 10620-10624.
35. K. Huang, G.-N. Wang, Y. Dai, Y.-T. Wu, X.-B. Hu and Z.-B. Zhang, *RSC Advances*, 2013, **3**, 16264.
36. K. Huang, Y.-L. Chen, X.-M. Zhang, S. Xia, Y.-T. Wu and X.-B. Hu, *Chem Eng J*, 2014, **237**, 478-486.
37. S. Tian, Y. Hou, W. Wu, S. Ren and C. Zhang, *RSC Adv*, 2013, **3**, 3572-3577.
38. K. Y. Lee, H. S. Kim, C. S. Kim and K.-D. Jung, *Int J Hydrogen Energ*, 2010, **35**, 10173-10178.
39. G. Qu, J. Zhang, J. Li and P. Ning, *Separ Sci Technol*, 2013, **48**, 2876-2879.
40. L. Zhang, Z. Zhang, Y. Sun, B. Jiang, X. Li, X. Ge and J. Wang, *Ind Eng Chem Res*, 2013, **52**, 16335-16340.
41. S. Y. Hong, J. Im, J. Palgunadi, S. D. Lee, J. S. Lee, H. S. Kim, M. Cheong and K.-D. Jung, *Energy Environ Sci*, 2011, **4**, 1802-1806.
42. W. Z. Wu, B. X. Han, H. X. Gao, Z. M. Liu, T. Jiang and J. Huang, *Angew Chem Int Ed*, 2004, **43**, 2415-2417.
43. Y. Shang, H. Li, S. Zhang, H. Xu, Z. Wang, L. Zhang and J. Zhang, *Chem Eng J*, 2011, **175**, 324-329.
44. S. Tang, G. A. Baker and H. Zhao, *Chem Soc Rev*, 2012, **41**, 4030.
45. Z. J. Chen, T. Xue and J.-M. Lee, *RSC Advances*, 2012, **2**, 10564.
46. J. L. Anderson, J. K. Dixon and J. F. Brennecke, *Accounts Chem Res*, 2007, **40**, 1208-1216.
47. T. K. Carlisle, J. E. Bara, C. J. Gabriel, R. D. Noble and D. L. Gin, *Ind Eng Chem Res*, 2008, **47**, 7005-7012.
48. Q. Zhang, Z. Li, J. Zhang, S. Zhang, L. Zhu, J. Yang, X. Zhang and Y. Deng, *J Phys Chem B*, 2007, **111**, 2864-2872.
49. C. M. Wang, J. J. Zheng, G. K. Cui, X. Y. Luo, Y. Guo and H. R. Li, *Chem Commun*, 2013, **49**, 1166-1168.
50. R. Steudel and Y. Steudel, *Eur J Inorg Chem*, 2007, 4385-4392.
51. J. J. Oh, M. S. Labarge, J. Matos, J. W. Kampf, K. W. Hillig and R. L. Kuczkowski, *J Am Chem Soc*, 1991, **113**, 4732-4738.
52. T. M. Townsend, A. Allanic, C. Noonan and J. R. Sodeau, *The Journal of Physical Chemistry A*, 2012, **116**, 4035-4046.
53. V. Vchirawongkwin, C. Pornpiganon, C. Kritayakornupong, A. Tongraar and B. M. Rode, *The Journal of Physical Chemistry B*, 2012, **116**, 11498-11507.
54. Z. Zhang, Y. Xie, W. Li, S. Hu, J. Song, T. Jiang and B. Han, *Angewandte Chemie International Edition*, 2008, **47**, 1127-1129.